ISSN 1674-1056
http://cpb.iphy.ac.cn
http://iopscience.iop.org/cpb
中国物理 B
Chinese Physics
中国物理
Chinese Physics B

Backward rescattered photoelectron holography in strong-field ionization

Fujun Chen(陈富军), Ruxian Yao(姚汝贤), Jianghua Luo(罗江华), Changqing Wang(王长清)
Citation: Chin. Phys. B . 2018, 27(10): 103202. **doi:** 10.1088/1674-1056/27/10/103202

Journal homepage: http://cpb.iphy.ac.cn; http://iopscience.iop.org/cpb

What follows is a list of articles you may be interested in

Interpulse interference of electron emission from an atom irradiated by sinusoidally phase-modulated pulse

Hai-Ying Yuan(袁海颖), Fu-Ming Guo(郭福明), Di-Yu Zhang(张崭玉), Jun Wang(王俊), Ji-Gen Chen(陈基根), Yu-Jun Yang(杨玉军)
Chin. Phys. B . 2018, 27(10): 103201. **doi:** 10.1088/1674-1056/27/10/103201

Effect of elliptical polarizations on nonsequential double ionization in two-color elliptically polarized laser fields

Tong-Tong Xu(徐彤彤), Jia-He Chen(陈佳贺), Xue-Fei Pan(潘雪飞), Hong-Dan Zhang(张宏丹), Shuai Ben(贲帅), Xue-Shen Liu(刘学深)
Chin. Phys. B . 2018, 27(9): 093201. **doi:** 10.1088/1674-1056/27/9/093201

Numerical tests of theoretical models describing ionization of H(1s) atom by linearly polarized flat pulse of laser radiation

Jarosław H Bauer, Min Deng(邓敏)
Chin. Phys. B . 2018, 27(9): 093202. **doi:** 10.1088/1674-1056/27/9/093202

Simultaneous study of the lower order harmonic and photoelectron emission from an atom in intense laser pulse

Yan Yan(闫妍), Fu-Ming Guo(郭福明), Jun Wang(王俊), Ji-Gen Chen(陈基根), Yu-Jun Yang(杨玉军)
Chin. Phys. B . 2018, 27(8): 083202. **doi:** 10.1088/1674-1056/27/8/083202

High-order harmonic generation in a two-color strong laser field with Bohmian trajectory theory

Yi-Yi Huang(黄祎祎), Xuan-Yang Lai(赖炫扬), Xiao-Jun Liu(柳晓军)
Chin. Phys. B . 2018, 27(7): 073204. **doi:** 10.1088/1674-1056/27/7/073204

Backward rescattered photoelectron holography in strong-field ionization*

Fujun Chen(陈富军)[1], Ruxian Yao(姚汝贤)[1], Jianghua Luo(罗江华)[2,3,†], and Changqing Wang(王长清)[4]

[1] School of Information Engineering, Huanghuai University, Zhumadian 463000, China
[2] School of Physics and Optoelectronic Engineering, Yangtze University, Jingzhou 434023, China
[3] Zhongshan Zhongchuang Technology Research Institute of Opto-electronics Industry, Zhongshan 528415, China
[4] Key Laboratory Optoelectronic Sensing Integrated Application of Henan Province, School of Electronic and Electrical Engineering, Henan Normal University, Xinxiang 453007, China

(Received 23 June 2018; revised manuscript received 11 August 2018; published online 10 September 2018)

By numerically solving the time-dependent Schrödinger equation, we observe a remarkable strong-field interference pattern in the photoelectron momentum distribution of a hydrogen atom ionized by a few-cycles laser pulse. This interference pattern is joined together with the familiar near-forward strong-field photoelectron holographic interference. By applying the strong-field approximation theory, we investigate the formation of this interference pattern, which arises from the interference between the backward rescattered part and the direct part of the tunneling ionized electron wave packet. We demonstrate that this backward rescattered photoelectron holographic interference can also be observed in a more realistic parallel two-color laser field. These results pave a new way to look into the atomic and molecular structure with ultrafast timescale.

Keywords: femtosecond physics, strong-field ionization, photoelectron holography

PACS: 32.80.Rm, 42.50.Hz, 32.80.Fb **DOI:** 10.1088/1674-1056/27/10/103202

1. Introduction

When an atom or molecule is exposed to a strong laser field, the electron in a bound state may be tunneling ionized through the barrier formed by the Coulomb potential of the parent ion and the electric field of the laser pulse, which is the basis of other strong-field processes.[1–9] During the laser pulse, the electron wave packets (EWP) ionized at different times with the same final momentum will interfere with each other due to the coherent nature. Therefore, various interference patterns appear in the final photoelectron momentum distribution (PMD). After tunneling ionization, the electron can be freed directly or driven back and recattered with the parent ion. For the direct electron, the interference pattern can be classified into two categories, i.e., intercycle and intracycle interferences. An intercycle interference pattern is formed by the EWPs tunneling ionized at different laser cycles, which has a ring-like pattern and is known as above-threshold ionization (ATI) peaks.[10,11] Intracycle interference is formed by the EWPs launched within a single period of the optical field.[12,13] By using a sculpted laser field, these interference patterns can be distinguished in the PMD[14–16] and serve as tools to retrieve the information about both the laser field and the parent ion.

The rescattered electron which is accelerated by the oscillation laser field and rescattered off the parent ion, may have the same final momentum as the direct electron, leading to the familiar strong-field photoelectron holographic interference in the PMD.[17–21] In this interference, the direct EWP acts as the reference wave and the rescattered electron acts as the signal wave, by analogy to the optical holography.[17] The strong field photoelectron holography (SFPH) records valuable structural information about the parent ion[22] and dynamical information about the valence electron.[23,24] For the near-forward scattered electron, the formed SFPH pattern appears with a fork-like structure in the PMD, which can be easily observed in experiments. In the previous works, one can extract the inherent structural information of the atoms and molecules, i.e., the phase of the scattering amplitude, from these holographic fringes.[20,25] Recently, an observation of the valence electron migration within the molecule with attosecond temporal resolution and angstrom spatial resolution using the previously proposed near-forward SFPH.[21] However, for the near-forward holographic interference, the rescattered electron only encodes the out range of the Coulomb potential and thus it lost some structural information about the parent ion. So that the backward rescattered photoelectron (BRP) holography is required to probe the structural information about the core.[26] In this work, by exploiting a few-cycle laser field, we find an interesting interference pattern in the PMD that was obtained by numerically solving the two-dimensional time-dependent

*Project supported by the Key Science and Technology Research of Henan Province, China (Grant Nos. 162102210111 and 172102310471) and the National Key Research and Development Program of China (Grant No. 2017YFB0403502).

†Corresponding author. E-mail: 87585705@qq.com

© 2018 Chinese Physical Society and IOP Publishing Ltd

Schrödinger equation (TDSE). This kind of interference stripe is confirmed to be the BRP holographic interference using the strong-field approximation (SFA) model. Further, we demonstrate that this BRP holographic structure can be observed with a more realistic sculpted laser field, encouraging experimental attempts on observing and decoding information from this holographic pattern.

2. Methods

To investigation the interference structure in the PMD, we numerically solve the TDSE for the hydrogen atom (atomic unit a.u. is used)

$$\mathrm{i}\frac{\partial}{\partial t}\Psi(\boldsymbol{r},t)=\mathcal{H}(\boldsymbol{r},t)\Psi(\boldsymbol{r},t), \tag{1}$$

with the Hamiltonian of the system $\mathcal{H}(\boldsymbol{r},t)=-\frac{1}{2}\nabla^2+V(r)+\boldsymbol{r}\cdot\boldsymbol{E}(t)$ in length gauge, where $\boldsymbol{r}=(x,y)$ in the two-dimensional space. $V(r)$ is the effective soft-core potential of the hydrogen atom:

$$V(r)=-\frac{1}{\sqrt{x^2+y^2+a}}. \tag{2}$$

Here the soft-core parameter $a=0.64$ to remove the Coulomb singularity and correctly reproduce the ground-state energy of the hydrogen atom. $\boldsymbol{E}(t)$ is the electric field used in our calculation with a $\sin^2(\pi t/\tau)$ form pulse envelope, where τ is the duration of this laser pulse. We also use a more realisitic Gaussian form envelope, and the resulting PMD is the same. First, we employ a linearly polarized laser pulse with the wavelength of 800 nm and the intensity of 1.0×10^{14} W/cm^2 as can be seen in Fig. 1(a). The duration of the laser field is $\tau=2T$ (T is the optical cycle period of the 800-nm pulse). The propagation of the wavefunction is continued for an additional six cycles after the end the laser pulse to collect slow photoelectrons. The TDSE is numerically solved by using the split-operator method[27,28] on a Cartesian grid ranging from -400 a.u. to 400 a.u. with a grid size of $\Delta x=\Delta y=0.1$ a.u. for both direction.

3. Results and discussion

The calculated PMD is presented in Fig. 1(b). Several kinds of interference patterns can be seen in the PMD. The clear fork-like stripes that distribute along the horizontal axis P_x form the near-forward SFPH. Another clear interference pattern is an arc-like structure with $P_x<0$ which is joined together with the fork-like stripes. We believe that these fringes originate from the interference between the direct electron and backward rescattered electron ionized at the instants indicated by the black arrows in Fig. 1(a). As can be seen, the vector potential possesses the same absolute value at these instants. Note that the duration of the laser pulse used in our calculation is extremely short, so that the intercycle interference[10] and the intracycle interference[12] patterns are disappeared in the PMD.

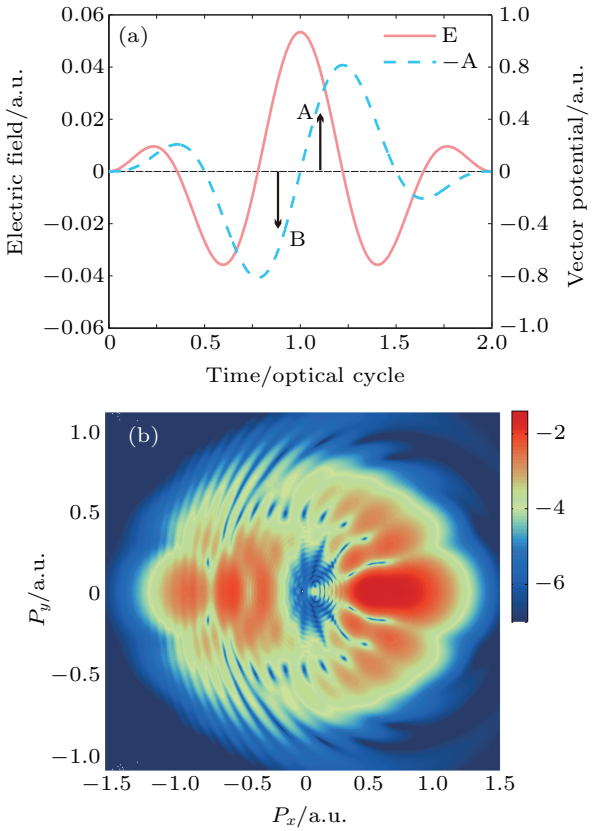


Fig. 1. (color online) (a) The electric field (red solid curve) and corresponding vector potential (blue dashed curve) of the few cycle laser field. The intensity of the 800-nm laser field is 1.0×10^{14} W/cm^2. The duration of the laser pulse is $\tau=2T$ (T is the optical cycle period of the 800-nm pulse). The black arrows A and B indicate the ionization time of the direct electron and rescattered electron that form the backward rescattered photoelectron hologram, respectively. (b) The simulated photoelectron momentum distribution of the hydrogen atom ionized by the laser pulse in panel (a), obtained by numerically solving a time-dependent Schrödinger equation.

To confirm that the arc-like pattern is the BRP holographic structure, we adopt the generalized SFA[17,29] to investigate the interferences in the PMD. Within the standard SFA, the strong field ionization process is described by the transition amplitude from the field-free bound state ψ_0 with ionization potential I_p to the Volkov state. For the direct electron, it reads

$$M_\mathrm{pi}^\mathrm{D}=-\mathrm{i}\int_0^t \mathrm{d}t'\langle\boldsymbol{p}+\boldsymbol{A}(t')|\boldsymbol{E}(t')\cdot\boldsymbol{r}|\psi_0\rangle\,\mathrm{e}^{-\mathrm{i}S_\mathrm{D}}, \tag{3}$$

where the classical action is

$$S_\mathrm{D}=\frac{1}{2}\int_{t'}^t \mathrm{d}\tau[\boldsymbol{p}+\boldsymbol{A}(\tau)]^2-I_\mathrm{p}t'. \tag{4}$$

For the rescattered electron, the transition amplitude reads

$$M_\mathrm{pi}^\mathrm{R}=-\int_0^t \mathrm{d}t'\int_{t'}^t \mathrm{d}t''\langle\boldsymbol{p}+\boldsymbol{A}(t'')|V(\boldsymbol{r})|\boldsymbol{k}+\boldsymbol{A}(t'')\rangle \times\langle\boldsymbol{k}+\boldsymbol{A}(t')|\boldsymbol{E}(t')\cdot\boldsymbol{r}|\psi_0\rangle\,\mathrm{e}^{-\mathrm{i}S_\mathrm{R}} \tag{5}$$

with the classical action

$$S_{\rm R} = \frac{1}{2}\int_{t'}^{t_r} {\rm d}\tau[\boldsymbol{k}+\boldsymbol{A}(\tau)]^2 + \frac{1}{2}\int_{t_r}^{t} {\rm d}\tau[\boldsymbol{p}+\boldsymbol{A}(\tau)]^2 - I_p t'. \quad (6)$$

In the above equations, $\boldsymbol{p}$ is the canonical potential, $\boldsymbol{A}(t) = -\int_0^t {\rm d}t'\boldsymbol{E}(t')$ is the vector potential of the laser fields, and t is the departing time of the laser pulse. To avoid the complexity of the five-dimensional integration over ionization times, the intermediate momentum $\boldsymbol{k}$ and the rescattering times t_r, we apply the saddle-point method to solve the transition amplitude.[30] Aditionally, in order to avoid the well-known divergence problem of the near-forward rescattering amplitude, the pre-factors in Eq. (5) are omitted, which is known to be a correct and effective way to reproduce the shape of interference stripes within the framework of SFA. Then, by calculating the total transition amplitude $M_{\rm pi} = M_{\rm pi}^{\rm D} + M_{\rm pi}^{\rm R}$, we are able to investigate the interference between the direct and the rescattered electrons.

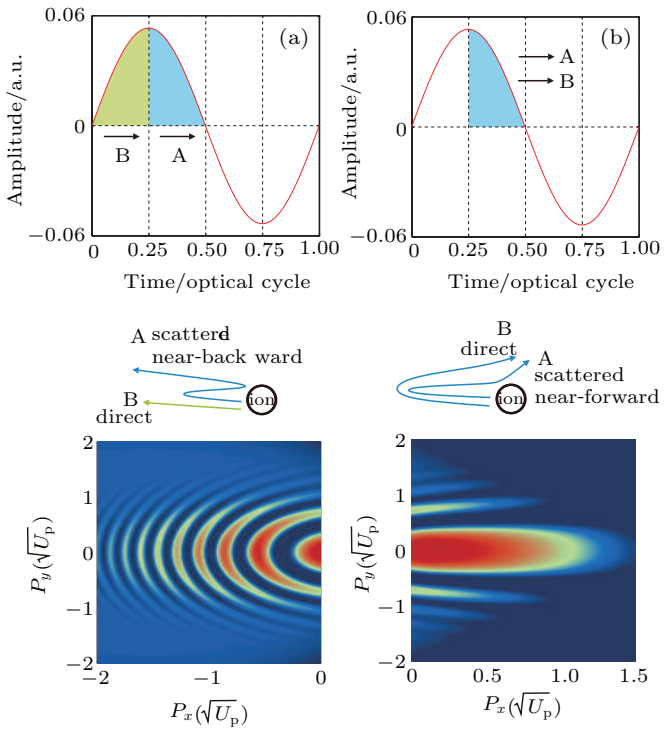


Fig. 2. (color online) Sketch for the near-forward rescattered photoelectron hologram (a) and the backward rescattered photoelectron hologram (b). The upper row presents the ionization time for the electron wave packets involved in the corresponding interference. The middle row presents the corresponding electron trajectories of the electron wave packets. The bottom row shows the interference structure simulated by strong-field approximation.

The simulated interference pattern with SFA is presented in Fig. 2. For the BRP holographic fringes, the direct electron and the backward rescattered electron are ionized at adjacent quarter cycles and start their motion on the same sides of the ion. The interference between these electrons forms an arc-like interference structure with final longitudinal momentum $P_x < 0$, as one can see in the bottom row of Fig. 2(a). As a comparison, in Fig. 2(b), we present the near-forward SFPH pattern simulated by generalized SFA. Different from the PRP holographic interference, here the direct electron and near-forward rescattered electron are liberated at the same quarter cycle. Their trajectories can be seen in the middle row of Fig. 2(b), which form the fork-like interference structure with final longitudinal momentum $P_x > 0$ presented in the bottom row. One can see that the forward and backward rescattered photoelectron holographic interference patterns can be joined together and form a complete rescattered electron interference pattern, since they are corresponding to the saddle point method solutions for rescattered electrons with a scattering angle less than 90° and larger than 90°, respectively.

By now, we have confirmed that the arc-like interference fringes in Fig. 1(b) are the backward interference structure, which are joined together with the familiar fork-like near-forward SFPH pattern. Owing to the two-cycle laser field, there are no complex interference structures that obscure the BRP holographic pattern, making it possible to easily identify this interference in PMD. We would like to emphasize that the carrier envelope phase (CEP) of the few-cycle laser pulse plays a important role to reveal the BRP holographic interference. In the present case, the CEP should be fixed near zero to suppress the intracycle interference. We have found that the BRP holographic interference fringes can still be resolved in the PMD after averaging the CEP of the laser pulse varying within [0, 0.12π]. We numerically tested that when the variation of CEP is larger than 0.15π, the BRP hologram will be smeared out and this strategy will be destroyed. Thus it is very challenging in experiments. In the following we employ a sculpted two-color laser pulse to emphasis the BRP holographic interference and attenuate other kinds of stripes, e.g., the intercycle interference, that may overlap the BRP interference.

As shown in Fig. 3(a), we use a parallel two-color laser field that is composed by 800-nm and 400-nm few-cycle laser pulses with the same intensity 1.0×10^{14} W/cm^2 to ionize the hydrogen atom. Here the duration of this two-color laser field is $\tau = 5T$ (T is the optical cycle period of the 800-nm pulse). The electric field for this laser pulse is indicated by the red curve, which is sculpted by the 400-nm laser field (compared with the one-color laser field), and thus provides an efficient control of the interference patterns. For example, we can barely see the near-forward interference in the region of $P_x < 0$ in Fig. 3(b), which is similar with that of the few-cycle linearly polarized one-color laser field. Without complex interference fringes that entangle with each other, in the PMD shown in Fig. 3(b), we clearly see the fork-like near-forward SFPH pattern and the arc-like BRP holographic fringes. An intuitive

explaination of revealing BRP interference using a two-color laser field can be given. For a single-color laser pulse with long duration, the BRP interference is hard to be observed in the PMD, because the shape of BRP interference is very similar with the intracycle interference between direct electrons and the signal of BRP interference is weaker than the intracycle interference. Generally, the signal of BRP interference is buried below and is not observable. In order to reveal it, the intracycle interference should be suppressed. The two-color laser field can achieve this goal. The intracycle interference originates from the interference between direct electrons liberated in adjacent half cycles, which can be viewed as a time-domain double-slit interference. In a two-color laser field, by adjusting the relative phase, the main peak of the electric field is enhanced and the side peaks are suppressed, as shown in Fig. 3(a). In the language of double-slit interference, the second color laser pulse with a proper choice of relative phase can switch off one of the time slit and thereby turn off the intracycle interference. In this way, the BRP interference can be clearly revealed, as shown in Fig. 3(b). Therefore, with a sculpted laser pulse, one can observe this BRP interference structure and employ it to investigate the structural information of the atom/molecule[20] in a further step.

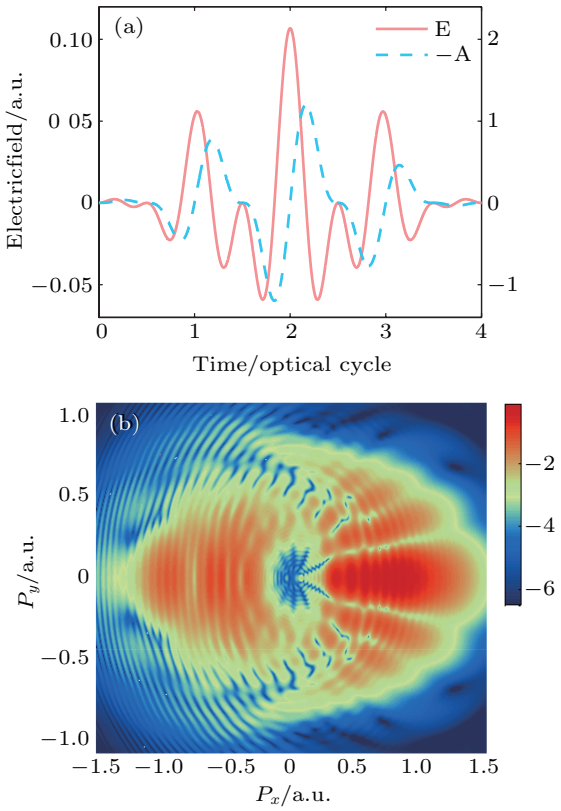


Fig. 3. (color online) (a) The electric field (red solid curve) and corresponding vector potential (blue dashed curve) of the sculpted two-color laser field that composed by 800-nm and 400-nm laser field with the same intensity 1.0×10^{14} W/cm^2. The duration of the two-color laser field is $\tau = 5T$ (T is the optical cycle period of the 800-nm pulse). (b) Corresponding photoelectron momentum distribution.

4. Conclusion

In conclusion, we theoretically investigate the holographic interference structure originating from the coherent interference between the backward rescattered electron wave packet and the direct electron wave packet by numerically solving the time-dependent Schrödinger equation. By employing a two-cycle infrared laser pulse, we investigate the ionization of the hydrogen atom, and find an arc-like interference structure in the obtained PMD, which is joined together with the fork-like near-forward SFPH. With the help of the generalized SFA method, we study the formation and appearance of the rescattering based interference structures and confirm that the arc-like stripes are the BRP holographic pattern. In a further step, we exam the appearance of these BRP interference fringes with an experimentally realistic laser pulse. By sculpting the laser pulse with a parallel second harmonic frequency laser pulse with comparable intensity, interference patterns that may obscure the BRP holographic fringes are attenuated and the clear BRP interference pattern appears in the PMD. It provides a practical method to get the information deep inside the potential of the targets and decode the electronic dynamics in future investigations.

References

[1] Becker W, Grasbon F, Kopold R, Milošević D B, Paulus G G and Walther H 2002 *Adv. At. Mol. Opt. Phys.* **48** 35
[2] Krausz F and Ivanov M 2009 *Rev. Mod. Phys.* **81** 163
[3] Zeng Z N, Wu J S and Jia Z M 2017 *Chin. Phys. B* **26** 093201
[4] Xia C L, Zhang J, Miao X Y and Liu X S 2017 *Chin. Phys. B* **26** 073201
[5] Lan P F, Ruhmann M, He L X, Zhai C Y, Wang F, Zhu X S, Zhang Q B, Zhou Y M, Li M, Lein M and Lu P X 2017 *Phys. Rev. Lett.* **119** 33201
[6] Zhou Y M, Huang C, Liao Q and Lu P X 2012 *Phys. Rev. Lett.* **109** 053004
[7] Chen Y B, Zhou Y M, Li Y, Li M, Lan P F and Lu P X 2018 *Phys. Rev. A* **97** 013428
[8] He L X, Zhang Q B, Lan P F, Cao W, Zhu X S, Zhai C Y, Wang F, Shi W J, Li M, Bian X B, Lu P X and Bandrauk A D 2018 *Nat. Commun.* **9** 1108
[9] Li L, Lan P F, He L X, Zhu X S, Chen J and Lu P X 2018 *Phys. Rev. Lett.* **120** 223203
[10] Agostini P, Fabre F, Mainfray G, Petite G and Rahman N K 1979 *Phys. Rev. Lett.* **42** 1127
[11] Tan J, Li Y, Zhou Y M, He M R, Chen Y B, Li M and Lu P X 2018 *Opt. Quantum Electron.* **50** 57
[12] Lindner F, Schätzel M G, Walther H, Baltuška A, Goulielmakis E, Krausz F, Milošević D B, Bauer D, Becker W and Paulus G G 2005 *Phys. Rev. Lett.* **95** 040401
[13] Arbó D G, Ishikawa K L, Schiessl K, Persson E and Burgdörfer J 2010 *Phys. Rev. A* **82** 043426
[14] Xie X H, Roither S, Kartashov D, Persson E, Arbó D G, Zhang L, Gräfe S, Schöffler M, Burgdörfer J, Baltuška A and Kitzler M 2012 *Phys. Rev. Lett.* **108** 193004
[15] Xie X H 2015 *Phys. Rev. Lett.* **114** 173003
[16] Richter M, Kunitski M, Schöffler M, Jahnke T, Schmidt L P H, Li M, Liu Y Q and Dörner R 2015 *Phys. Rev. Lett.* **114** 143001
[17] Huismans Y, Rouzée A, Gijsbertsen A, Jungmann J, Smolkowska A, Logman P, Lépine F, Cauchy C, Zamith S, Marchenko T, Bakker J, Berden G, Redlich B, van der Meer A, Muller H, Vermin W, Schafer K, Spanner M, Ivanov M, Smirnova O, Bauer D, Popruzhenko S and Vrakking M 2011 *Science* **331** 61

[18] Bian X B, Huismans Y, Smirnova O, Yuan K J, Vrakking M and Bandrauk A D 2011 *Phys. Rev. A* **84** 043420

[19] He M R, Zhou Y M, Li Y, Li M and Lu P X 2016 *Phys. Rev. A* **93** 033406

[20] Xie H, Li M, Luo S Q, Li Y, Tan J, Zhou Y M, Cao W and Lu P X 2018 *Opt. Lett.* **43** 3220

[21] He M R, Li Y, Zhou Y M, Li M, Cao W and Lu P X 2018 *Phys. Rev. Lett.* **120** 133204

[22] Hickstein D, Ranitovic P, Witte S, Tong X, Huismans Y, Arpin P, Zhou X, Keister K, Hogle C, Zhang B, Ding C, Johnsson P, Toshima N, Vrakking M, Murnane M and Kapteyn H 2012 *Phys. Rev. Lett.* **109** 073004

[23] Meckel M, Staudte A, Patchkovskii S, Villeneuve D M, Corkum P B, Dörner R and M. Spanner 2014 *Nat. Phys.* **10** 594

[24] Walt S, Ram N, Atala M, Shvetsov-Shilovski N, Conta A, Baykusheva D, Lein M and Wörner H 2017 *Nat. Commun.* **8** 15651

[25] Zhou Y M, Tolstikhin O and Morishita T 2016 *Phys. Rev. Lett.* **116** 173001

[26] Haertelt M, Bian X, Spanner M, Staudte A and Corkum P B 2016 *Phys. Rev. Lett.* **116** 133001

[27] Feit M D, Fleck J A and Steiger A 1982 *J. Comput. Phys.* **47** 412

[28] Tong X M, Hino K and Toshima N 2006 *Phys. Rev. A* **74** 031405

[29] Huismans Y, Gijsbertsen A, Smolkowska A, Jungmann J, Rouzée A, Logman P, Lépine F, Cauchy C, Zamith S, Marchenko T, Bakker J, Berden G, Redlich B, van der Meer A F G, Ivanov M, Yan T, Bauer D, Smirnova O and M. Vrakking 2012 *Phys. Rev. Lett.* **109** 013002

[30] Salières P, Carré B, Déroff L Le, Grasbon F, Paulus G G, Walther H, Kopold R, Becker W, Milošević D B, Sanpera A and Lewenstein M 2001 *Science* **292** 902